Kovove Mater. 57 2019 121–129
DOI: 10.4149/km_2019_1_121

Cr cluster characterization in Cu-Cr-Zr alloy after ECAP processing and aging using SANS and HAADF-STEM

K. Abib[1]*, H. Azzeddine[1,2], B. Alili[1], L. Lityńska-Dobrzyńska[3], A. L. Helbert[4], T. Baudin[4], P. Jegou[5], M. H. Mathon[5], P. Zieba[3], D. Bradai[1]

[1] *Faculty of Physics, University of Sciences and Technology Houari Boumediene, BP 32 El Alia, 16111 Bab Ezzouar, Algiers, Algeria*
[2] *Department of Physics, University Mohamed Boudiaf, 28000 M'sila, Algeria*
[3] *Institute of Metallurgy and Materials Science, Polish Academy of Sciences, 25 Reymonta St., 30059 Krakow, Poland*
[4] *ICMMO, SP2M, Univ. Paris-Sud, University Paris-Saclay, UMR CNRS 28182, 91405 Orsay Cedex, France*
[5] *Laboratoire Léon Brillouin, CEA-CNRS, CEA/Saclay, 91191 Gif-sur-Yvette, France*

Received 3 November 2018, received in revised form 5 February 2019, accepted 19 February 2019

Abstract

The precipitation of nano-sized Cr clusters was investigated in a commercial Cu-1Cr-0.1Zr (wt.%) alloy processed by equal-channel angular pressing and subsequent aging at 550 °C for 4 h using Small-Angle Neutron Scattering (SANS) measurements and High-Angle Annular Dark-Field-Scanning Transmission Electron Microscopy (HAADF-STEM). The size and volume fraction of the nano-sized Cr clusters were estimated using both techniques. The parameter values assessed by SANS ($d \sim 3.2$ nm, $F_v \sim 1.1$ %) agreed reasonably with those by HAADF-STEM ($d \sim 2.5$ nm, $F_v \sim 2.3$ %). In addition to the nano-sized Cr clusters, HAADF--STEM indicated the presence of rare cuboid and spheroid sub-micronic Cr particles measuring approximately 380–620 nm in mean size. Both techniques did not evidence the presence of intermetallic Cu_xZr_y phases within the aging conditions.

K e y w o r d s: Cr-cluster, precipitation, ECAP, Cu-Cr-Zr alloy, SANS, HAADF-STEM

1. Introduction

Cu-Cr-Zr alloys are the subject of many research activities owing to their potential use in industrial and technological areas, such as electric/microelectronics and nuclear fusion reactors [1]. The high conductivity of these alloys is mainly attributed to the low solubility of Cr and Zr in Cu at room temperature [2], whereas their strength is due to the precipitation of Cr clusters and Cu_xZr_y phases in Cu matrices [3, 4]. However, many authors have reported antagonist findings of the sequence and nature of precipitates that can appear during annealing after conventional or severe plastic deformation (SPD) of Cu-Cr-Zr alloys [5–16]. Besides Cr clusters, different Cu_xZr_y phases have been found in Cu-Cr-Zr alloys: orthorhombic Cu_4Zr phase [10, 17] and $Cu_{51}Zr_{14}$ (believed to be Cu_3Zr) phase [11]. More complicated phases, such as Cu_7Cr_3ZrSi and $CrCu_2$(Zr, Mg) Heusler phases have also been observed [18–20]. It was reported in binary Cu-Cr and Cu-Zr and in ternary Cu-Cr-Zr alloys that Cr precipitates appeared first at about 440 °C, followed by separate Cu_3Zr precipitation at approximately 520 °C [21]. A similar sequence was reported in Cu-Cr-Zr alloys that were severely deformed by equal-channel angular pressing (ECAP) [5, 22].

The substantial influence of SPD processes, such as ECAP and high-pressure torsion (HPT), on the structure, precipitation sequence, thermal stability, and mechanical properties of Cu-based alloys has been the object of many studies [5, 21–29]. The processing of alloys by SPD produces significant grain refinement and a high density of dislocations and vacancies [30]. These characteristics enhance the mobility of solute species, generate additional nucleation sites for precipitations, and consequently strongly modify their kinetics [24, 30].

After ECAP processing, the grains of Cu-Cr-Zr al-

*Corresponding author: e-mail address: abib_khadidja@yahoo.com

loys were strongly refined to 1 μm concomitant with high dislocation densities and significant hardness enhancement of up to 250 % [5, 22, 23, 27, 31]. Purcek et al. [27, 31] showed that among the different ECAP routes, route Bc was found to generate the smallest grain size and the highest hardness and strength [27]. Moreover, post-ECAP aging led to precipitation hardened ultrafine grain structure that remained stable under both thermal and mechanical conditions [5].

Since the pioneering work of Vinogradov et al. [5], very few studies have been devoted to the chemical and microstructural changes, precipitate nature and morphology, and precipitation sequence that may occur during and/or after SPD processing of Cu-Cr-Zr alloys.

Hatakeyama et al. [18] and Chbihi et al. [32] reported quantitative data of size distribution, volume fraction, and other morphological features of Cr clusters in Cu-Cr-Zr alloys without any prior deformation by using TEM and 3D-atom probe tomography (3D--ATP). They evidenced the existence of nano-scaled Cr precipitates with a spherical, plate, and ellipsoid shapes and sizes ranging between 2 and 50 nm.

Small-angle neutron scattering (SANS) and high-angle annular dark-field scanning transmission electron microscopy (HAADF-STEM) are powerful tools for determining the size distribution and volume fraction of precipitates in materials and alloys. Contrary to microscopic techniques, SANS analyzes a relatively large volume and thus provides average values over a very large number of precipitates; thus, this method is highly sensitive to small changes in the size and volume fraction of precipitates [33].

The present study aims to comparatively evaluate the size distribution and the volume fraction of precipitates in a Cu-1Cr-0.1Zr (wt.%) alloy after SPD processing by ECAP and aging at 550 ℃ for 4 h using SANS and HAADF-STEM.

2. Experimental procedure

The material considered in this study was a commercial Cu-1Cr-0.1Zr (wt.%) alloy that was supplied in the form of rod bars by Good Fellow (UK). Billets of 10 mm diameter and 60 mm length were then machined for ECAP processing and then solution heat-treated for 1 h at 1 040 ℃ in a protective inert gas atmosphere, followed by water quenching. The rods were then processed by ECAP at room temperature up to one pass using route B_c. Full details of the ECAP processing can be found in [34, 35]. This route was specially chosen for generating a fine equiaxed microstructure with a high volume fraction of high-angle grain boundaries [31]. After ECAP processing, annealing was conducted at 550 ℃ for 4 h under high vacuum.

Analytical transmission electron microscope FEI Tecnai G2, at 200 kV and equipped with an HAADF--STEM detector and an energy-dispersive X-ray spectrometer (EDS), was employed for microstructural (ultrafine grain size, precipitate size distribution, their nature, and volume fraction) characterization of the Cu-1Cr-0.1Zr alloy after various heat treatments. The TEM specimens were electro-polished using a TenuPol-5 twinjet polishing unit with an electrolyte of 75 % CH_3OH and 25 % HNO_3. In the HAADF--STEM experiments, six was the spot size used (approximately 1 nm beam diameter). The volume fraction of the precipitates was estimated using Scion Image for Windows. The area values of a selected number of precipitates in a TEM micrograph were computed and divided by the frame in which they were selected. Since all the sections of the thin foil perpendicular to the view plan were equivalent, the surface fraction was assumed equal to the volume fraction. Five TEM micrographs were used, as suggested by DeHoff and Rhines [36].

The SANS experiments were performed on a PAXY spectrometer in the Orphée reactor at the Laboratoire Léon Brillouin (CEA-CNRS, Saclay, France, Proposal N° 12796). Two configurations of incident wavelength and sample-detector distance were used: 0.6 nm and 2 m; 0.9 nm and 5 m. The total covered scattering range was then $0.01 < q < 2\,\mathrm{nm}^{-1}$. Data were normalized and corrected for sample transmission and sample holder contribution. From the obtained 2D patterns, the SANS intensities (I) were deduced. The analysis method (of the $\log(I)$ vs. q plots) used for estimating the precipitate size and volume fraction is discussed in detail in [37, 38].

Following this method, the SANS intensity per unit volume is given by:

$$I(q) = \Delta\rho^2 N_\mathrm{p} V_\mathrm{p}^2 F(q) s(q), \tag{1}$$

where N_p and V_p are the number density and volume of particles, respectively. $\Delta\rho$ is the nuclear contrast and is written as:

$$\Delta\rho = \frac{b^p}{v_\mathrm{at}^p} - \frac{b^m}{v_\mathrm{at}^m}, \tag{2}$$

where $b^{p,m}$ and $v_\mathrm{at}^{p,m}$ are the average scattering length and average atomic volume in the precipitate (p) or the matrix (m), respectively. $F(q)$ is the form factor of the particles and $S(q)$ the structure factor (in the present study, the volume fraction is of the order of 1–2 %, so $S(q)$ is assumed equal to 1). The precipitates are supposed spherical with a radius R, and the corresponding form factor is:

$$F(q,R) = \left[3\frac{\sin(qr) - qr\cos(qr)}{(qr)^3}\right]^2. \tag{3}$$

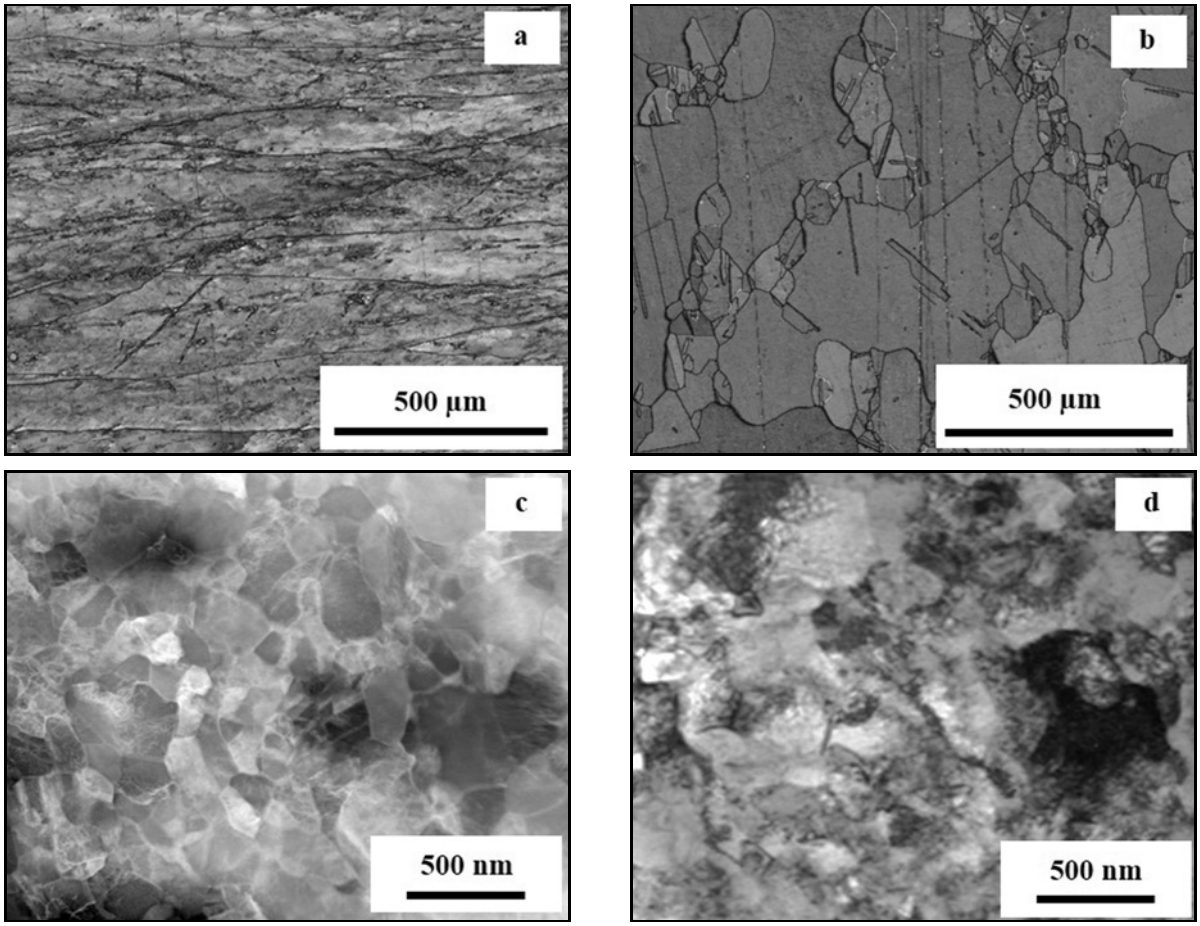

Fig. 1. The microstructure of Cu-1Cr-0.1Zr (wt.%) alloy: (a) as received, (b) solution annealed at 1 040 °C for 1 h, (c) HAADF-STEM, and (d) TEM bright field image after ECAP processing to 1 pass and aging at 550 °C for 4 h.

Furthermore, the precipitates are not monodisperse, and the size distribution has to be considered. In this case, the Gaussian size distribution was taken into account for the data analysis. The Gaussian distribution is given by:

$$h(R) = \frac{1}{\sqrt{2\pi\sigma}} \left[-\frac{(R - R_{\mathrm{m}})^2}{2\sigma^2} \right]^2, \qquad (4)$$

where R_{m} is the mean radius. The half-width of the size distribution at half maximum is $\Delta R = \sqrt{2 \ln 2}\sigma = 1.177\sigma$. Under these assumptions, Eq. (1) is rewritten as:

$$I(q) = \Delta\rho^2 f_{\mathrm{v}} \frac{\int_0^\infty h(R)\, V_{\mathrm{p}}^2 F(q,R)\, \mathrm{d}R}{\int_0^\infty h(R)\, V_{\mathrm{p}} \mathrm{d}R}, \qquad (5)$$

where f_{v} is the volume fraction of the particles.

3. Results and discussion

Figure 1 shows the microstructure of the Cu-Cr-Zr alloy in the as-received state (Fig. 1a) after solution heat treatment at 1 040 °C for 1 h (Fig. 1b), one pass of ECAP processing, and subsequent aging at 550 °C for 4 h (Figs. 1c–d). Figs. 1a and b were reproduced from EBSD maps in the Index of Quality format [35].

As already reported in [35], the microstructure of the as-received alloy is characterized by the presence of long parallel elongated grains in fibrous form. This columnar structure with an average transverse grain size of approximately 130 µm resulted from strong thermal gradients during casting. Figure 1b shows a coarse equiaxed granular microstructure that resulted after solution annealing at 1 040 °C for 1 h in an Ar atmosphere. This heating led to a grain mean diameter of approximately 100 µm, which is larger than that reported by Purcek et al. [31] for a similar alloy that underwent solution annealing at 1 020 °C for 20 min. This grain size difference is remarkable owing to noticeable grain growth that may occur under increased temperatures and annealing times. Grain boundaries are irregular, and many annealing twins are present in the microstructure.

As observed in Fig. 1c, ECAP processing to one pass and annealing at 550 °C for 4 h resulted in a typical microstructure consisting of ultrafine sub-grains with an average grain size of about 200 ± 40 nm, as

estimated by the linear intercept method, in which all grains separated by both high-angle and low-angle grain boundaries were considered.

This sub-grain size is very close to that reported by Purcek et al. [31] for a Cu-0.8Cr-0.08Zr (wt.%) alloy after eight passes of the ECAP technique. These authors stated that the grain size and morphology did not considerably change between four and eight ECAP passes.

Hence, it can be stipulated that the sub-grain size saturates soon after one ECAP pass and up to 16 passes. Figure 1b suggests that neither normal nor abnormal grain growth is observed in the aged alloy. A surprising absence of any effect of aging at 450 ℃ for 1 h on the morphology and grain size of ECAPed Cu--0.80Cr-0.080Zr (wt.%) alloy was reported by Purcek et al. [27, 31]. Vinogradov et al. [5] also demonstrated the impressive fact that the ECAP structure remained fine-grained during the heating and aging of a Cu--0.44Cr-0.2Zr (wt.%) alloy at temperatures reaching 600 ℃. This persistent UFG microstructure may be due to its effective stabilization by the Cr cluster and/or Cu_5Zr particles [8].

Enhanced magnification shows that the microstructure (Fig. 1d) consists of dislocation-free sub-grains with sharp (high-angle) boundaries and zones of moderate-to-high distortions and dislocation walls (low-angle boundaries). Many grain boundaries are not apparent due to the existence of high dislocation density in their vicinity. Many similar observations were reported in the literature after SPD processing and aging of Cu-based alloys [5, 28, 31].

Normally, annealing under such conditions should result in substantial recrystallization and grain growth. Previous work demonstrated that a Cu-1Cr-0.1Zr (wt.%) alloy exhibited good thermal stability of up to 550 ℃ after ECAP processing and annealing [22].

An interesting finding is the presence of quasi-cuboid and quasi-spheroid sub-micronic particles in the microstructure of the annealed Cu-Cr-Zr alloy, as shown in Figs. 2a,b. The sizes of the cuboid and spheroid particles are approximately 380 and 620 nm, respectively.

Table 1 summarizes the results of point EDS analysis of the Cu matrix and the cuboid and spheroid particles, which correspond to analyzed zones 1, 2, and 3, respectively. The two particles are composed of ∼ 98 % Cr and 2 % Cu. No trace of Zr is detected in the core of the spheroid particle. The selected area diffraction (SAD) pattern taken from Fig. 2b inside the sub-micronic precipitate is shown in Fig. 2c. The key to Fig. 2c (zone axis [111]), which shows the position of fundamental reflections from the Cr cluster, which are superimposed on the spots in Fig. 2c, confirms the presence of only a Cr bcc phase with a lattice parameter of 0.288 nm.

Aside from the rare sub-micronic particles in the microstructure, profuse nano-sized particles can be noticed inside the sub-grains, as demonstrated in Fig. 3. Highly similar observations were reported in the literature [5, 12, 32, 39, 40]. In these reports, such particles were identified as Cr clusters. Unfortunately, the

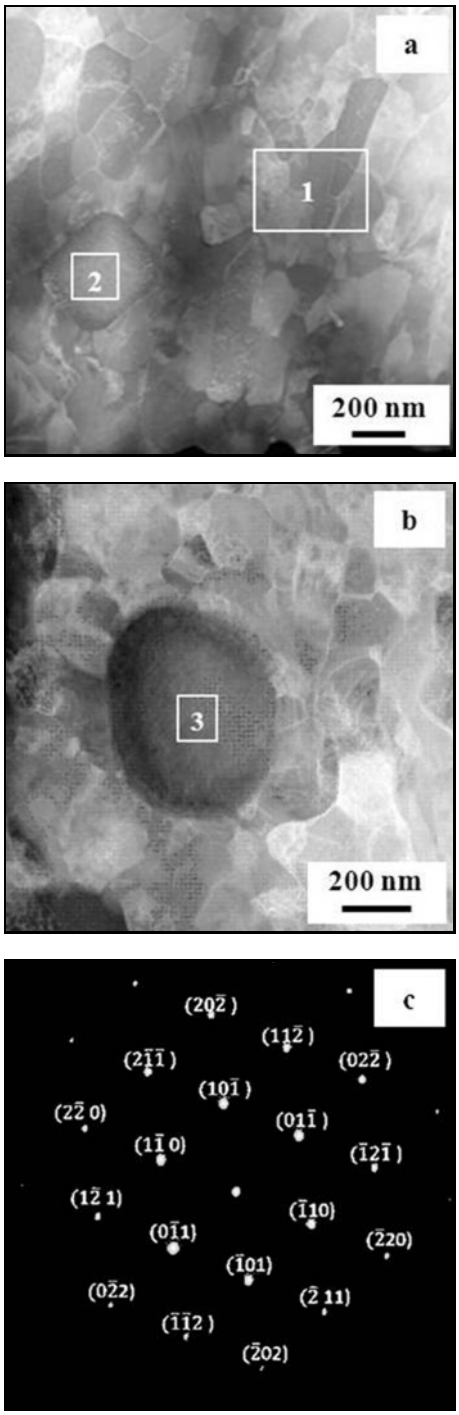

Fig. 2. HAADF-STEM images of: (a) cuboid and (b) spheroid sub-micronic Cr clusters, (c) Selected Area Diffraction (SAD) pattern taken from Fig. 1b inside the sub-micronic spheroid cluster.

Table 1. EDS analysis of Cu matrix, cuboid, and spheroid particles

Element	Cu matrix (wt.%)	Cuboid particle (wt.%)	Spheroid particle (wt.%)
Cr(K)	0. 2	97.4	97.4
Cu(K)	99.7	2.5	2.5
Zr(K)	0.1	0.03	–

Table 2. SANS Cr precipitation characterization on homogenized and ECAP deformed Cu-1Cr-0.1Zr alloy and annealed at 550 °C for 4 h, respectively

Sample	Mean radius (nm)	Standard deviation	F_v (%)
Reference	1.1	0.2	1.1
ECAP-1 Pass + 4 h at 550 °C	1.6	0.5	1.1

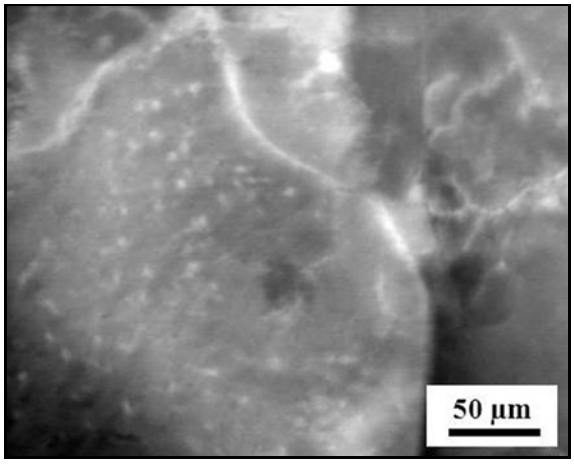

Fig. 3. HAADF-STEM image showing nano-sized Cr clusters (in white contrast) within one sub-grain of deformed Cu-Cr-Zr alloy after annealing at 550 °C for 4 h.

present work failed to perform EDS analysis because the precipitates were very small (few nanometers) compared to the foil thickness (usually approximately 50 nm). Hence, the EDS signal should be strongly convoluted between the particles and the matrix lying under and above the particles. Vinogradov et al. [5] reported that the precipitation of a fine Cr cluster started after aging at 375 °C for 15 h. The morphology and size of such clusters did not change appreciably and later remained in a diameter range of 5–20 nm even after aging at 425 and 500 °C [5]. Meanwhile, it was reported that Cr clusters could be transformed into large and stable bcc particles at higher temperatures (500 °C) and longer annealing times (two days) [38].

The precipitation nature and sequence in Cu-Cr-Zr alloys after thermomechanical processing have been thoroughly studied [5–16]; by contrast, the presence of similar sub-micronic Cr clusters has been reported in only a few studies [12, 41, 42]. Using energy-dispersive spectroscopy (EDS) mapping, Zhang et al. [42] showed that sub-micronic Cr clusters had a core-shell structure with the shell of Zr and the core of Cr. These relatively coarse phases are thought to form during solidification and are left undissolved during the solution [43]. The growth of the coarse Cr phase in as-cast ingot prefers certain orientations [12]. The SANS technique failed to detect them within the explored q range in this study due to their relatively large size and very low volume fraction.

The nuclear scattering intensities measured on the deformed Cu-Cr-Zr alloy and annealed at 550 °C for 4h are shown in Fig. 4. Data from homogenized (unprocessed and un-aged) Cu-1Cr-0.1Zr alloys as a reference sample were also given for comparison. The nuclear scattering intensities of the deformed Cu-1Cr-0.1Zr alloy and annealed at 550 °C for 4 h exhibit a weak, extended, and broad peak in the range of $0.375 < q < 1.40\,\mathrm{nm}^{-1}$ compared with the reference sample.

The SANS data show that at a small q, the intensity decreases rapidly, following a slope in q^{-4}. This is consistent with the behavior of Porod, which is the signature of the microstructure of a polycrystalline material with or without very large particles. The Porod behavior is the same for the reference and the ECAPed and aged sample; the microstructure (grains, grain boundaries, or very large particles) was not modified by the last thermomechanical treatment. At a high angle, that in the reference sample has an additional contribution due to nano-objects; this contribution is much higher in the deformed and annealed material than in the reference. The measured scattered intensities were fitted assuming a Porod law and a Gaussian size distribution of small spherical or ellipsoidal particles. The agreement between the experimental and calculated data is excellent, as illustrated by the right side of Fig. 4. The results of the data fitting are summarized in Table 2. Meanwhile, the evaluation of the precipitated volume fraction F_v from the experimen-

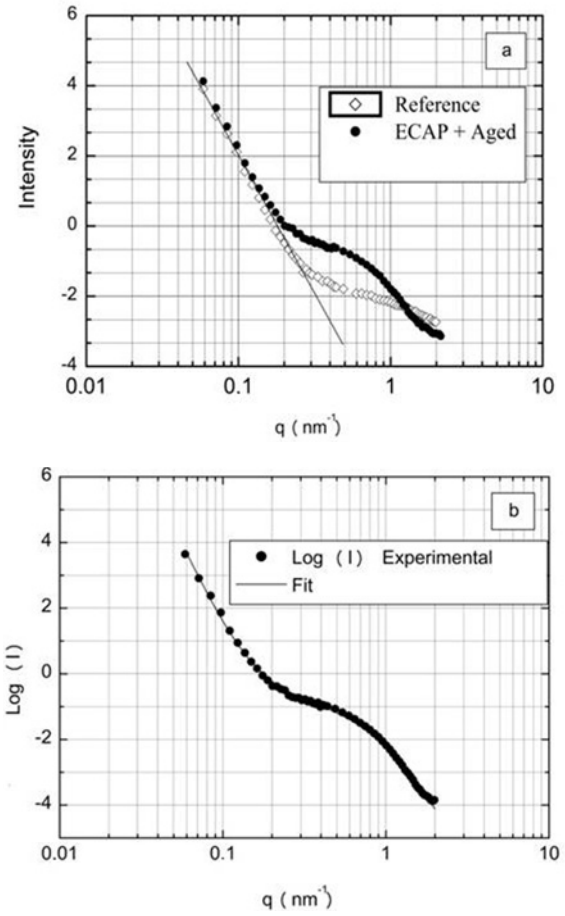

Fig. 4. (a) Nuclear scattering intensities for homogenized and deformed Cu-1Cr-0.1Zr alloy and annealed at 550 °C for 4 h, respectively. The continuous line illustrates the Porod behavior (I vs. $(1/q^4)$) attempted for alloy without nano-particles and (b) example of data adjustment obtained on the higher intensity.

Table 3. Estimation of size (diameter) and volume fraction of Cr nanocluster from SANS and HAADF-STEM analysis of deformed Cu-Cr-Zr alloy after annealing at 550 °C for 4 h

Diameter (nm)		F_v (%)	
SANS	HAADF	SANS	HAADF
3.2	2.5	1.1	2.3

tal data fit requires knowledge of the nuclear contrast and thus the chemical composition. In this case, the precipitates were considered pure Cr.

The results confirm that in the reference state, approximately 1 % of very small particles already exist. In the annealed sample, the size of the precipitates shows a clear increase, reaching a radius of 1.6 nm. The volume fraction is constant. Meanwhile, the size and volume fraction of the Cr nano-clusters were estimated by quantitative metallography from a set of HAADF-STEM micrographs (Fig. 3, for example) and then compiled with those found by SANS in Table 3. Both SANS and HAADF-STEM allowed the assessment of the size and volume fraction of the Cr clusters with reasonable accuracy and agreement.

In the literature, there is controversy about the effect of long solution annealing on the Cr dissolution in the Cu matrix of Cu-Cr-Zr alloys. Indeed, many authors [18, 23, 44, 45] stated that Cu-Cr-Zr, after solution annealing in the range of 930–1 050 °C, becomes fully free from any precipitate or cluster. Other studies [12, 43, 46] evidenced the presence of Cr clusters caused by incomplete dissolution. The present results confirm the fact that SANS is a powerful method that is very sensitive to small variations in the nano-objects size.

The size of the Cr cluster (diameter 3.3–2.5 nm), as determined by SANS and HAADF-STEM, falls within the range of those assessed by many authors [12, 18, 39, 40]. The volume fraction found by SANS is in agreement with the initial Cr content of the alloys, indicating the precipitation of all Cr atoms. The F_v value determined by TEM is higher but remains in the same order of magnitude, albeit in the error bars of this technique. It is interesting to note that Chbihi et al. [32], using EDS mapping in STEM mode, estimated the Cr cluster volume fraction to be in the range of 0.86–1.3 %. Surprisingly, both techniques did not evidence any presence of other types of precipitation. The use of 3D-AP and TEM techniques has demonstrated the presence of only bcc Cr clusters having probably Nishiyama-Wassermann (N-W) orientation relation after aging at 460 °C for 3 h and even after prolonged aging at 600 °C for 5 h of Cu-Cr-Zr alloys [20]. Chbihi et al. [32] and Li et al. [40] also reported the existence of only Cr clusters. Li et al. [40] identified them as having an ordered fcc with a cube-on-cube relationship with the Cu matrix. From exhaustive TEM characterization, Chbihi et al. [32] stated that three kinds of Cr clusters might coexist. Some of them were fcc and coherent with the matrix, whereas others were probably bcc with either N-W or Kurdjumov-Sachs (K-S) orientation relation.

Based on TEM and 3D-APT, Chbihi et al. [32] widely discussed the nucleation and growth of Cr clusters and proposed the following probable precipitation sequence: (i) nucleation of coherent fcc spherical precipitates, (ii) growth and transformation of fcc spherical precipitates into bcc structure, and (iii) growth of bcc precipitates with K-S OR at the expense of those with N-W OR.

Hence precipitation of the Cr-rich equilibrium bcc phase was thought to initiate through the nucleation of fcc precipitates that are coherent with the Cu-rich

fcc parent phase. Very similar precipitation scenario has been reported in age-hardenable Al alloys [32]. Recently, it has also been demonstrated that the ordered fcc Cr phase is the precursor to the formation of the bcc phase in Cu-Cr-Zr alloys [32].

The nature and morphology of intermetallic compounds that can form in Cu-Cr-Zr systems have been considered to be linked to the local concentration of Zr. Intermetallics, such as Cu_8Zr_3, $Cu_{51}Zr_{14}$, Cu_4Zr, and Cu_5Zr, and Heusler phases type ($CrCu_2$(Zr, Mg)) [19, 20] may precipitate in such systems. However, a close inspection of the published data revealed a preponderance of $Cu_{51}Zr_{14}$ compound with Cr content below 1 % [12]. Such intermetallic particles generally have a larger size ($d = 10$–30 nm) than Cr precipitates [43]. Besides Cr clusters, a Cu_5Zr phase with a quite smaller size ($d < 5$ nm) that precipitated preferentially at twin boundaries, sub-grain boundaries, and within the twin/matrix lamellae was observed by Li et al. [40]. These findings were in good agreement with previous observations of Holzwarth et al. [9] and Fuxiang et al. [47]. However, as mentioned above, Li et al. [40] recently reported the presence of only a Cr cluster. It is worth noting that both SANS and HAADF-STEM can obtain the conclusion of the existence but not the absence of precipitation with small size and small volume fraction.

The formation of Cu_xZr_y (mainly $Cu_{51}Zr_{14}$ and Cu_5Zr) should normally be enhanced after SPD. For example, ECAP can induce mutation in microstructure in a scale of grains and in precipitation, which can deviate greatly from paths that are observed in traditional processes. SPD can be considered "hot deformation at room temperature," that is, a balance between deformation-induced grain refinement and deformation-accelerated formation of equilibrium phases [48]. However, paradoxical inverse trends have also been reported in the literature. One of these processes reported in some experimental works is the spectacular cementite dissolution after [49] HPT.

It has also been reported that ECAP has a relatively complicated effect on the evolution of precipitates, and this effect is strongly dependent on the initial state of the Al alloy and the deformation temperature [50]. Pre-existing precipitated phases may dissolve, and supersaturated solid solutions may also form [50]. Straumal et al. [51] reviewed the possible effects of SPD processing on phase transformation. They stated that the phases before and after SPD differed. SPD can drive the formation or decomposition of a supersaturated solid solution; dissolution of phases; disordering of ordered phases; amorphization of crystalline phases; synthesis of low-temperature, high-temperature, or high-pressure allotropic modifications; and nanocrystallization in amorphous matrices.

Ongoing complementary studies will be accomplished to thoroughly investigate the entire nature and sequence of Cr clusters and precipitation and their evolution upon the aging of Cu-Cr-Zr systems after SPD by ECAP up to high strains.

4. Conclusions

On the basis of the experimental results, the following conclusions are drawn:

– Cu-1Cr-0.1Zr alloy exhibits excellent thermal stability up to 550 ℃ after ECAP processing and annealing with an average grain size of approximately 160 nm.

– HAADF-STEM indicates the presence of cuboid and spheroid sub-micronic particles measuring about 380 and 620 nm, respectively.

– The size and volume fraction of the nano-sized Cr clusters estimated using SANS technique ($d \sim 3.2$ nm, $F_v \sim 1.1$ %) agrees reasonably with those determined by HAADF-STEM one ($d \sim 2.5$ nm, $F_v \sim 2.3$ %).

– The nano-precipitation of Cu_xZr_y is not observed after ECAP processing and aging.

Acknowledgements

The authors wish to heartily thank Prof. Jose Maria Cabrera from ETSEIB, Universidad Politécnica de Cataluña, for inviting and helping Miss K. Abib during her several scientific stays. This work was supported in part by the international PHC-MAGHREB Program No. 16MAG03.

References

[1] Edwards, D. J., Singh, B. N., Tähtinen, S.: J. Nucl. Mater., *367–370*, 2007, p. 904. doi:10.1016/j.jnucmat.2007.03.064

[2] Batra, I. S., Dey, G. K., Kulkarni, U. D., Banerjee, S.: J. Nucl. Mater., *299*, 2001, p. 91. doi:10.1016/S0022-3115(01)00691-2

[3] Batra, I. S., Dey, G. K., Kulkarni, U. D., Banerjee, S.: Mater. Sci. Eng. A, *356*, 2002, p. 32. doi:10.1016/S0921-5093(02)00852-3

[4] Fuxiang, H., Jusheng, M., Honglong, N., Zhiting, G., Chao, L., Shumei, G., Xuetao, Y., Tao, W., Hong, L., Huafen, L.: Scr. Mater., *48*, 2003, p. 97. doi:10.1016/S1359-6462(02)00353-6

[5] Vinogradov, A., Patlan, V., Suzuki, Y., Kitagawa, K., Kopylov, V. I.: Acta Mater., *50*, 2002, p. 1639. doi:10.1016/S1359-6454(01)00437-2

[6] Zhang, Y., Volinsky, A. A., Tran, H. T., Chai, Z., Liu, P., Tian, B., Liu, Y.: Mater. Sci. Eng. A, *650*, 2016, p. 248. doi:10.1016/j.msea.2015.10.046

[7] Kvačkaj, T., Bidulský, R., Kováčová, A., Ileninová, J., Bidulská, J.: Acta Metallurgica Slovaca, *20*, 2014, p. 397. doi:10.12776/ams.v20i4.438

[8] Shangina, D. V., Bochvar, N. R., Morozova, A. I., Belyakov, A. N., Kaibyshev, R. O., Dobatkin, S. V.: Mater. Lett., *199*, 2017, p. 46. doi:10.1016/j.matlet.2017.04.039
[9] Holzwarth, U., Stamm, H.: J. Nucl. Mater., *279*, 2000, p. 31. doi:10.1016/S0022-3115(99)00285-8
[10] Tang, N. Y., Taplin, D. M. R., Dunlop, G. L.: Mater. Sci. Technol., *1*, 1985, p. 270. doi:10.1179/mst.1985.1.4.270
[11] Liu, P., Kang, B. X., Gao, X. G., Huang, J. L., Yen, B., Gu, H. C.: Mater. Sci. Eng. A, *265*, 1999, p. 262. doi:10.1016/S0921-5093(98)01149-6
[12] Li, H., Shuisheng, X., Xujun, M., Pengyue, W.: J. Mater. Sci. Technol., *23*, 2007, p. 795.
[13] Xia, C. D., Jia, Y. L., Zhang, W., Zhang, K., Dong, Q. Y., Xu, G. Y., Wang, M.: Mater. Des., *39*, 2012, p. 404. doi:10.1016/j.matdes.2012.03.003
[14] Mu, S. G., Guo, F. A., Tang, Y. Q., Cao, X. M., Tang, M. T.: Mater. Sci. Eng. A, *475*, 2008, p. 235. doi:10.1016/j.msea.2007.04.056
[15] Liu, P., Kang, B. X., Cao, X. G., Huang, J. L., Yen, B., Gu, H. C.: Mater. Sci. Eng. A, *265*, 1999, p. 262. doi:10.1016/S0921-5093(98)01149-6
[16] Su, J. H., Liu, P., Dong, Q. M., Li, H. J., Ren, F. Z., Tian, B. H.: J. Mater. Eng. Perform., *16*, 2007, p. 490. doi:10.1007/s11665-007-9071-x
[17] Wang, Q. J., Liu, F., Du, Z. Z., Wang, J. Y.: Chin. J. Rare Met., *37*, 2013, p. 687. doi:10.1007/s11665-007-9071-x
[18] Hatakeyama, M., Toyama, T., Yang, J., Nagai, Y., Hasegawa, M., Ohkubo, T., Eldrup, M., Singh, B. N.: J. Nucl. Mater., *386–388*, 2009, p. 852. doi:10.1016/j.jnucmat.2008.12.266
[19] Tu, J. P., Qi, W. X., Liu, F.: Wear, *49*, 2002, p. 1021. doi:10.1016/S0043-1648(01)00843-2
[20] Qi, W. X., Tu, J. P., Liu, F., Yang, Y. Z., Wang, N. Y., Lu, H. M., Zhang, X. B., Guo, S. Y., Liu, M. S.: Mater. Sci. Eng. A Struct., *343*, 2003, p. 89. doi:10.1016/S0921-5093(02)00387-8
[21] Vinogradov, A., Suzuki, Y., Ishida, T., Kitagawa, K., Kopylov, V. I.: Mater. Trans., *45*, 2004, p. 2187. doi:10.2320/matertrans.45.2187
[22] Abib, K., Azzeddine, H., Tirsatine, K., Baudin, T., Helbert, A. L., Brisset, F., Alili, B., Bradai, D.: Mater. Charact., *118*, 2016, p. 527. doi:10.1016/j.matchar.2016.07.006
[23] Vinogradov, A., Kitagawa, K., Kopylov, V. I.: Mater. Sci. Forum, *503–504*, 2006, p. 811. doi:10.4028/www.scientific.net/MSF.503-504.811
[24] Azzeddine, H., Mehdi, B., Hennet, L., Thiaudiere, D., Alili, B., Kawasaki, M., Bradai, D., Langdon, T. G.: Mater. Sci. Eng. A, *597*, 2014, p. 288. doi:10.1016/j.msea.2013.12.092
[25] Wei, K. X., Wei, W., Wang, F., Du, Q. B., Alexandrov, I. V., Hu, J.: Mater. Sci. Eng. A, *528*, 2011, p. 1478. doi:10.1016/j.msea.2010.10.059
[26] León, K. V., Muñoz-Morris, M. A., Morris, D. G.: Mater Sci. Eng. A, *536*, 2012, p. 181. doi:10.1016/j.msea.2011.12.098
[27] Purcek, G., Yanar, H., Demirtas, M., Alemdag, Y., Shangina, D. V., Dobatkin, S. V.: Mater. Sci. Eng. A, *649*, 2016, p. 114. doi:10.1016/j.msea.2015.09.111
[28] Shangina, D. V., Gubicza, J., Dodony, E., Bochvar, N. R., Straumal, P. B., Tabachkova, N. Y., Dobatkin, S. V.: J. Mater. Sci., *49*, 2014, p. 6674. doi:10.1007/s10853-014-8339-4
[29] Purcek, G., Yanar, H., Shangina, D. V., Demirtas, M., Bochvar, N. R., Dobatkin, S. V.: J. Alloys Compd., *742*, 2018, p. 325. doi:10.1016/j.jallcom.2018.01.303
[30] Zehetbauer, M. J., Zhu, Y. T. (Eds.): Bulk Nanostructured Materials. Weinheim, Wiley-VCH 2009.
[31] Purcek, G., Yanar, H., Saray, O., Karaman, I., Maier, H. J.: Wear, *311*, 2014, p. 149. doi:10.1016/j.wear.2014.01.007
[32] Chbihi, A., Sauvage, X., Blavette, D.: Acta Materialia, *60*, 2012, p. 4575. doi:10.1016/j.actamat.2012.01.038
[33] Staron, P., Eidenberger, E., Schober, M., Sharp, M., Leitner, H., Schreyer, A., Clemens, H.: Journal of Physics, Conference Series, *247*, 2010, p. 012038. doi:10.1088/1742-6596/247/1/012038
[34] Abib, K., HadjLarbi, F., Rabahi, L., Alili, B., Bradai, D.: Trans. Nonferrous Met. Soc. China, *25*, 2015, p. 838. doi:10.1016/S1003-6326(15)63671-8
[35] Abib, K., Balanos, J. A. M., Alili, B., Bradai, D.: Mater. Charact., *112*, 2016, p. 252. doi:10.1016/j.matchar.2015.12.026
[36] De Hoff, R. T., Rhines, F. N.: Quantitative Microscopy. New York, McGraw-Hill Book Co. 1968.
[37] Mathon, M. H., De Novion, C. H.: J. Physique IV, *9*, 1999, p. 127.
[38] Maître, A., Bourguignon, G., Medjahdi, G., McRae, E., Mathon, M. H.: Scr. Mater., *50*, 2004, p. 685. doi:10.1016/j.scriptamat.2003.11.013
[39] Chen, X., Jiang, F., Liu, L., Huang, H., Shi, Z.: Materials Science and Technology, *34*, 2017, p. 1. doi:10.1080/02670836.2017.1376428
[40] Li, R., Guo, E., Chen, Z., Kang, H., Wang, W., Zou, C., Li, T., Wang, T.: Journal of Alloys and Compounds, *771*, 2019, p. 1044. doi:10.1016/j.jallcom.2018.09.040
[41] Dybiec, H., Rdzawski, Z., Richert, M.: Mater. Sci. Eng. A, *108*, 1989, p. 97. doi:10.1016/0921-5093(89)90410-3
[42] Zhang, S. J., Li, R. G., Kang, H. J., Chen, Z. N., Wang, W., Zou, C. L., Li, T. J., Wang, T. M.: Mater. Sci. Eng. A, *680*, 2017, p. 108. doi:10.1016/j.msea.2016.10.087
[43] Mei, Z., Guobiao, L., Zidong, W., Maokui, Z.: China Foundry, *5*, 2008, p. 268.
[44] Islamgaliev, R. K., Nesterov, K. M., Champion, Y., Valiev, R. Z.: IOP Conf. Series: Materials Science and Engineering, *63*, 2014, p. 012118. doi:10.1088/1757-899X/63/1/012118
[45] Lipinska, M., Bazarnik, P., Lewandowska, M.: IOP Conf. Series: Materials Science and Engineering, *63*, 2014, p. 012119. doi:10.1088/1757-899X/63/1/012119
[46] Shuai, G., Zhang, M., Yan, Y.: Anal. Stereol., *23*, 2004, p. 137. doi:10.5566/ias.v23.p137-141
[47] Fuxiang, H., Jusheng, M., Honglong, N., Zhiting, G., Chao, L., Shumei, G., Xuetao, Y., Tao, W., Hong, L., Huafen, L.: Scr. Mater., *48*, 2003, p. 97. doi:10.1016/S1359-6462(02)00353-6
[48] Straumal, B. B., Mazilkin, A. A., Protasova, S. G., Dobatkin, S. V., Rodin, A. O., Baretzky, B., Goll, D., Schütz, G.: Mater. Sci. Eng. A, *503*, 2009, p. 185. doi:10.1016/j.msea.2008.03.052
[49] Ivanisenko, Y., Lojkovski, W., Valiev, R. Z., Fecht, H.

J.: Acta Mater., *51*, 2003, p. 5555. doi:10.1016/S1359-6454(03)00419-1

[50] Gazizov, M., Kaibyshev, R.: Mater. Sci. Eng. A, *588*, 2013, p. 65. doi:10.1016/j.msea.2013.09.021

[51] Straumal, B. B., Kilmametov, A. R., Ivanisenko, Y., Mazilkin, A. A., Kogtenkova, O. A., Kurmanaeva, L., Korneva, A., Zieba, P., Baretzky, B.: Int. J. Mater. Res. (formerly Z. Metallkd.), *106*, 2015, p. 658. doi:10.3139/146.111215